Chapter 4
Discontinuous Galerkin Methods for Metamaterials

In this chapter, we introduce several discontinuous Galerkin (DG) methods for solving time-dependent Maxwell's equations in dispersive media and metamaterials. We first present a succint review of DG methods in Sect. 4.1. Then we present some DG methods for the cold plasma model in Sect. 4.2. Here the DG methods are developed for a second-order integro-differential vector wave equation. We then consider DG methods for the Drude model written in a system of first-order differential equations in Sect. 4.3. Finally, we extend the nodal DG methods developed by Hesthaven and Warburton (Nodal discontinuous Galerkin methods: algorithms, analysis, and applications. Springer, New York, 2008) to metamaterial Maxwell's equations in Sect. 4.4.

4.1 A Brief Overview of DG Methods

The discontinuous Galerkin method was originally introduced in 1973 by Reed and Hill for solving a neutron transport equation. In recent years the DG method gained more popularity in solving various differential equations due to its great flexibility in mesh construction, easily handling complex geometries or interfaces, and efficiency in parallel implementation. A detailed overview on the evolution of the DG methods from 1973 to 1999 is provided by Cockburn et al. [83]. More details and references on DG methods can be found in books [83, 99, 141, 247] and references therein.

In the past decade, there has been considerable interest in developing DG methods for Maxwell's equations in the free space [70, 84, 100, 120, 133, 140, 147, 168, 219, 238]. However, the study of DG method for Maxwell's equations in dispersive media (including metamaterial, a lossy dispersive composite material) are very limited. In 2004, a time-domain DG method was investigated in [207] for solving the first-order Maxwell's equations in dispersive media, but no error analysis was carried out. In 2009, a priori error estimate [151] and a posteriori error estimation [182] of the interior penalty DG method were obtained for Maxwell's

J. Li and Y. Huang, *Time-Domain Finite Element Methods for Maxwell's Equations in Metamaterials*, Springer Series in Computational Mathematics 43,
DOI 10.1007/978-3-642-33789-5_4,

equations in dispersive media. However, the error estimate obtained in [151] was optimal in the energy norm, but sub-optimal in the L^2-norm. Later, the error estimates were improved to be optimal in the L^2-norm for both a semi-discrete DG scheme and a fully explicit DG scheme [186]. In [155], a fully implicit DG method was developed for solving dispersive media models. This scheme is proved to be unconditionally stable and has optimal error estimates in both L^2 norm and DG energy norm. Very recently, some DG methods have been developed for dispersive [251, 290] and metamaterial [185] Maxwell's equations written as a system of first-order differential equations.

4.2 Discontinuous Galerkin Methods for Cold Plasma

4.2.1 The Modeling Equations

It is known that in reality all electromagnetic media show some dispersion, i.e., some physical parameters such as permittivity (and/or permeability) depends on the wavelength. Such media are often called dispersive media. In most applications, we are interested in linear dispersive media, which satisfy the relation (cf. (1.11)):

$$\mathbf{D}(\mathbf{x}, t) = \epsilon(\omega)\mathbf{E}, \quad \mathbf{B}(\mathbf{x}, t) = \mu(\omega)\mathbf{E},$$

and are often encountered in nature. For example, rock, soil, ice, snow, and plasma are dispersive media. Hence, transient simulation of electromagnetic wave propagation and scattering in dispersive media is important for a wide range of applications involving biological media, optical materials, artificial dielectrics, or earth media, where the host medium is frequency dispersive.

Since early 1990s, many FDTD methods have been developed for modeling electromagnetic propagation in isotropic cold plasma. Early references can be found in Chap. 9 of [276]. It is known that for an isotropic nonmagnetized cold electron plasma, the complete governing equations are:

$$\epsilon_0 \frac{\partial \mathbf{E}}{\partial t} = \nabla \times \mathbf{H} - \tilde{\mathbf{J}} \tag{4.1}$$

$$\mu_0 \frac{\partial \mathbf{H}}{\partial t} = -\nabla \times \mathbf{E} \tag{4.2}$$

$$\frac{\partial \tilde{\mathbf{J}}}{\partial t} + \nu \tilde{\mathbf{J}} = \epsilon_0 \omega_p^2 \mathbf{E} \tag{4.3}$$

where $\mathbf{E}$ is the electric field, $\mathbf{H}$ is the magnetic field, ϵ_0 is the permittivity of free space, μ_0 is the permeability of free space, $\tilde{\mathbf{J}}$ is the polarization current density, ω_p is the plasma frequency, $\nu \geq 0$ is the electron-neutron collision frequency. Solving (4.3) with the assumption that the initial electron velocity is 0, we obtain

$$\tilde{\mathbf{J}}(\mathbf{E}) \equiv \tilde{\mathbf{J}}(\mathbf{x}, t; \mathbf{E})$$
$$= \epsilon_0 \omega_p^2 e^{-\nu t} \int_0^t e^{\nu s} \mathbf{E}(\mathbf{x}, s) ds = \epsilon_0 \omega_p^2 \int_0^t e^{-\nu(t-s)} \mathbf{E}(\mathbf{x}, s) ds. \quad (4.4)$$

Taking derivative of (4.1) with respect to t, and eliminating $\mathbf{H}$ and $\tilde{\mathbf{J}}$ by using (4.2)–(4.4), we can reduce the modeling equations to the following integro-differential equation

$$\mathbf{E}_{tt} + \nabla \times (C_v^2 \nabla \times \mathbf{E}) + \omega_p^2 \mathbf{E} - \mathbf{J}(\mathbf{E}) = 0 \quad \text{in } \Omega \times I, \quad (4.5)$$

where the rescaled polarization current density $\mathbf{J}$ is represented as

$$\mathbf{J}(\mathbf{E}) = \nu \omega_p^2 \int_0^t e^{-\nu(t-s)} \mathbf{E}(\mathbf{x}, s) ds. \quad (4.6)$$

Recall that $C_v = \frac{1}{\sqrt{\epsilon_0 \mu_0}}$ denotes the wave speed in free space. Here $I = (0, T)$ is a finite time interval and Ω is a bounded Lipschitz polyhedron in R^3.

To make the problem complete, we assume that the boundary of Ω is a perfect conductor so that

$$\mathbf{n} \times \mathbf{E} = \mathbf{0} \quad \text{on} \quad \partial\Omega \times I, \quad (4.7)$$

and the initial conditions for (4.5) are given as

$$\mathbf{E}(\mathbf{x}, 0) = \mathbf{E}_0(\mathbf{x}) \quad \text{and} \quad \mathbf{E}_t(\mathbf{x}, 0) = \mathbf{E}_1(\mathbf{x}), \quad (4.8)$$

where $\mathbf{E}_0(\mathbf{x})$ and $\mathbf{E}_1(\mathbf{x})$ are some given functions.

Lemma 4.1. *There exists a unique solution* $\mathbf{E} \in H_0(curl; \Omega)$ *for (4.5).*

Proof. Taking the Laplace transformation of (4.5) and denoting $\hat{\mathbf{E}}(s)$ as the Laplace transformation of $\mathbf{E}(t)$, we have

$$s^2 \hat{\mathbf{E}} - s\mathbf{E}(0) - \mathbf{E}_t(0) + \nabla \times (C_v^2 \nabla \times \hat{\mathbf{E}}) + \omega_p^2 \hat{\mathbf{E}} - \nu \omega_p^2 \frac{1}{s + \nu} \hat{\mathbf{E}} = 0,$$

which can be rewritten as

$$s(s^2 + \nu s + \omega_p^2)\hat{\mathbf{E}} + (s + \nu)\nabla \times (C_v^2 \nabla \times \hat{\mathbf{E}}) = s(s + \nu)\mathbf{E}(0) + (s + \nu)\mathbf{E}_t(0). \quad (4.9)$$

The weak formulation of (4.9) can be formulated as: Find $\hat{\mathbf{E}} \in H_0(\text{curl}; \Omega)$ such that

$$s(s^2 + \nu s + \omega_p^2)(\hat{\mathbf{E}}, \phi) + (s + \nu)(C_v^2 \nabla \times \hat{\mathbf{E}}, \nabla \times \phi)$$
$$= (s(s + \nu)\mathbf{E}(0) + (s + \nu)\mathbf{E}_t(0), \phi), \quad (4.10)$$

holds true for any $\phi \in H_0(\text{curl}; \Omega)$. The existence of a unique weak solution $\hat{\mathbf{E}}$ is guaranteed by the Lax-Milgram lemma. Taking the inverse Laplace transformation of $\hat{\mathbf{E}}$ leads to the solution $\mathbf{E}$ for (4.5). □

4.2.2 A Semi-discrete Scheme

We consider a shape-regular mesh T_h that partitions the domain Ω into disjoint tetrahedral elements $\{K\}$, such that $\overline{\Omega} = \bigcup_{K \in T_h} K$. Furthermore, we denote the set of all interior faces by F_h^I, the set of all boundary faces by F_h^B, and the set of all faces by $F_h = F_h^I \cup F_h^B$. We want to remark that the optimal L^2-norm error estimate is based on a duality argument and inverse estimate, hence we need to assume that the mesh be quasi-uniform and the domain Ω be convex.

We assume that the finite element space is given by

$$\mathbf{V}_h = \{\mathbf{v} \in L^2(\Omega)^3 : \ \mathbf{v}|_K \in (P_l(K))^3, \ K \in T_h\}, \ \ l \geq 1, \tag{4.11}$$

where $P_l(K)$ denotes the space of polynomials of total degree at most l on K.

A semi-discrete DG scheme can be formed for (4.5): For any $t \in (0, T)$, find $\mathbf{E}^h(\cdot, t) \in \mathbf{V}_h$ such that

$$(\mathbf{E}_{tt}^h, \phi) + a_h(\mathbf{E}^h, \phi) + \omega_p^2(\mathbf{E}^h, \phi) - (\mathbf{J}(\mathbf{E}^h), \phi) = 0, \ \ \forall\, \phi \in \mathbf{V}_h, \tag{4.12}$$

subject to the initial conditions

$$\mathbf{E}^h|_{t=0} = \Pi_2 \mathbf{E}_0, \quad \mathbf{E}_t^h|_{t=0} = \Pi_2 \mathbf{E}_1, \tag{4.13}$$

where Π_2 denotes the standard L_2-projection onto $\mathbf{V}_h$. Moreover, the bilinear form a_h is defined on $\mathbf{V}_h \times \mathbf{V}_h$ as

$$\begin{aligned} a_h(\mathbf{u}, \mathbf{v}) = & \sum_{K \in T_h} \int_K C_v^2 \nabla \times \mathbf{u} \cdot \nabla \times \mathbf{v} d\mathbf{x} - \sum_{f \in F_h} \int_f [[\mathbf{u}]]_T \cdot \{\{C_v^2 \nabla \times \mathbf{v}\}\} dA \\ & - \sum_{f \in F_h} \int_f [[\mathbf{v}]]_T \cdot \{\{C_v^2 \nabla \times \mathbf{u}\}\} dA + \sum_{f \in F_h} \int_f a [[\mathbf{u}]]_T \cdot [[\mathbf{v}]]_T dA. \end{aligned}$$

Here $[[\mathbf{v}]]_T$ and $\{\{\mathbf{v}\}\}$ are the standard notation for the tangential jumps and averages of $\mathbf{v}$ across an interior face $f = \partial K^+ \cap \partial K^-$ between two neighboring elements K^+ and K^-:

$$[[\mathbf{v}]]_T = \mathbf{n}^+ \times \mathbf{v}^+ + \mathbf{n}^- \times \mathbf{v}^-, \quad \{\{\mathbf{v}\}\} = (\mathbf{v}^+ + \mathbf{v}^-)/2, \tag{4.14}$$

where $\mathbf{v}^{\pm}$ denote the traces of $\mathbf{v}$ from within $K^{\pm}$, and $\mathbf{n}^{\pm}$ denote the unit outward normal vectors on the boundaries $\partial K^{\pm}$, respectively. While on a boundary face $f = \partial K \cap \partial \Omega$, we define $[[\mathbf{v}]]_T = \mathbf{n} \times \mathbf{v}$ and $\{\{\mathbf{v}\}\} = \mathbf{v}$. Finally, a is a penalty function, which is defined on each face $f \in F_h$ as:

$$a|_f = \gamma c_v^2 \hbar^{-1},$$

where $\hbar|_f = \min\{h_{K+}, h_{K-}\}$ for an interior face $f = \partial K^+ \cap \partial K^-$, and $\hbar|_f = h_K$ for a boundary face $f = \partial K \cap \partial \Omega$. The penalty parameter γ is a positive constant and has to be chosen sufficiently large in order to guarantee the coercivity of $\tilde{a}_h(\cdot, \cdot)$ defined below.

Furthermore, we denote the space $\mathbf{V}(h) = H_0(\text{curl}; \Omega) + \mathbf{V}_h$ and define the semi-norm

$$|\mathbf{v}|_h^2 = \sum_{K \in F_h} ||C_v \nabla \times \mathbf{v}||_{0,K}^2 + \sum_{f \in F_h} ||a^{1/2}[[\mathbf{v}]]_T||_{0,f}^2,$$

and the DG energy norm by

$$||\mathbf{v}||_h^2 = ||\omega_p \mathbf{v}||_{0,\Omega}^2 + |\mathbf{v}|_h^2.$$

In order to carry out the error analysis, we introduce an auxiliary bilinear form $\tilde{a}_h$ on $\mathbf{V}(h) \times \mathbf{V}(h)$ defined as [134]

$$\begin{aligned}\tilde{a}_h(\mathbf{u}, \mathbf{v}) = &\sum_{K \in T_h} \int_K C_v^2 \nabla \times \mathbf{u} \cdot \nabla \times \mathbf{v} d\mathbf{x} - \sum_{f \in F_h} \int_f [[\mathbf{u}]]_T \cdot \{\{C_v^2 \Pi_2(\nabla \times \mathbf{v})\}\} dA \\ &- \sum_{f \in F_h} \int_f [[\mathbf{v}]]_T \cdot \{\{C_v^2 \Pi_2(\nabla \times \mathbf{u})\}\} dA + \sum_{f \in F_h} \int_f a[[\mathbf{u}]]_T \cdot [[\mathbf{v}]]_T dA.\end{aligned}$$

Note that $\tilde{a}_h$ equals a_h on $\mathbf{V}_h \times \mathbf{V}_h$ and is well defined on $H_0(\text{curl}; \Omega) \times H_0(\text{curl}; \Omega)$.

It is shown that $\tilde{a}_h$ is both continuous and coersive:

Lemma 4.2 ([133, Lemma 5]). *For γ larger than a positive constant γ_{min}, independent of the local mesh sizes, we have*

$$|\tilde{a}_h(\mathbf{u}, \mathbf{v})| \leq C_{cont} |\mathbf{u}|_h |\mathbf{v}|_h, \quad \tilde{a}_h(\mathbf{v}, \mathbf{v}) \geq C_{coer} |\mathbf{v}|_h^2, \quad \mathbf{u}, \mathbf{v} \in \mathbf{V}(h),$$

where $C_{cont} = \sqrt{2}$ and $C_{coer} = \frac{1}{2}$.

For an element K and any $\mathbf{u} \in (P_l(K))^3$, we have the standard inverse estimate

$$||\nabla \times \mathbf{u}||_{0,K} \leq C h_K^{-1} ||\mathbf{u}||_{0,K},$$

and the trace estimate

$$||\mathbf{u}||_{0,\partial K} \leq C h_K^{-\frac{1}{2}} ||\mathbf{u}||_{0,K},$$

which, along with Lemma 4.2, yields the following lemma.

Lemma 4.3. *For a quasi-uniform mesh T_h, there holds*

$$|\tilde{a}_h(\mathbf{u},\mathbf{u})| \le C_b h^{-2}||\mathbf{u}||_0^2, \quad \mathbf{u} \in \mathbf{V}_h,$$

where the constant $C_b > 0$ depends on the quasi-uniformity constant of the mesh and polynomial degree l, but is independent of the mesh size h.

First, we can prove that (4.12) has a unique solution.

Lemma 4.4. *There exists a unique solution $\mathbf{E}^h$ for the discrete model (4.12).*

Proof. Choosing $\phi = \mathbf{E}_t^h$ in (4.12), we obtain

$$\frac{1}{2}\frac{d}{dt}(||\mathbf{E}_t^h||_0^2 + a_h(\mathbf{E}^h,\mathbf{E}^h) + \omega_p^2||\mathbf{E}^h||_0^2) - (\mathbf{J}(\mathbf{E}^h),\mathbf{E}_t^h) = 0,$$

integrating which, we have

$$\begin{aligned} &||\mathbf{E}_t^h(t)||_0^2 + a_h(\mathbf{E}^h(t),\mathbf{E}^h(t)) + \omega_p^2||\mathbf{E}^h(t)||_0^2 \\ &= ||\mathbf{E}_t^h(0)||_0^2 + a_h(\mathbf{E}^h(0),\mathbf{E}^h(0)) + \omega_p^2||\mathbf{E}^h(0)||_0^2 + 2\int_0^t (\mathbf{J}(\mathbf{E}^h),\mathbf{E}_t^h)dt. \end{aligned} \tag{4.15}$$

Using the Cauchy-Schwarz inequality and the definition of $\mathbf{J}(\mathbf{E})$, we have

$$\begin{aligned} 2\int_0^t (\mathbf{J}(\mathbf{E}^h),\mathbf{E}_t^h)dt &\le \int_0^t ||\mathbf{J}(\mathbf{E}^h(t))||_0^2 dt + \int_0^t ||\mathbf{E}_t^h(t)||_0^2 dt \\ &\le \int_0^t \frac{\nu\omega_p^4}{2}\int_0^t ||\mathbf{E}^h(s)||_0^2 ds dt + \int_0^t ||\mathbf{E}_t^h(t)||_0^2 dt \\ &\le \frac{\nu\omega_p^4 t}{2}\int_0^t ||\mathbf{E}^h(t)||_0^2 dt + \int_0^t ||\mathbf{E}_t^h(t)||_0^2 dt. \end{aligned}$$

Substituting the above estimate into (4.15), then using Lemma 4.2 and the discrete Gronwall inequality, we have the following stability

$$||\mathbf{E}_t^h(t)||_0^2 + |\mathbf{E}^h(t)|_h^2 + ||\mathbf{E}^h(t)||_0^2 \le ||\mathbf{E}_t^h(0)||_0^2 + |\mathbf{E}^h(0)|_h^2 + ||\mathbf{E}^h(0)||_0^2,$$

which implies the uniqueness of solution for (4.12). Since (4.12) is a finite dimensional linear system, the uniqueness of solution gives the existence immediately. □

The following optimal error estimate for (4.12) is proved in [186].

Theorem 4.1. *Let $\mathbf{E}$ and $\mathbf{E}^h$ be the solutions of (4.5) and (4.12), respectively. Then under the following regularity assumptions*

$$\mathbf{E},\mathbf{E}_t \in L^\infty(0,T;(H^{\alpha+\sigma_E}(\Omega))^3), \quad \nabla\times\mathbf{E},\nabla\times\mathbf{E}_t \in L^\infty(0,T;(H^\alpha(\Omega))^3), \forall\,\alpha > \frac{1}{2},$$

there holds

$$||\mathbf{E} - \mathbf{E}^h||_{L^\infty(0,T;(L^2(\Omega))^3)} \le C h^{\min(\alpha,l)+\sigma_E},$$

where $l \ge 1$ *is the degree of the polynomial function in the finite element space (4.11),* $\sigma_E \in (\frac{1}{2}, 1]$ *is related to the regularity of the Laplacian in polyhedra (*$\sigma_E = 1$ *when* Ω *is convex), and the constant* $C > 0$ *is independent of* h.

Note that when $\mathbf{E}$ is smooth enough on a convex domain, Theorem 4.1 gives the optimal error estimate in the L^2-norm:

$$||\mathbf{E} - \mathbf{E}^h||_{L^\infty(0,T;(L^2(\Omega))^3)} \le C h^{l+1}.$$

4.2.3 A Fully Explicit Scheme

To define a fully discrete scheme, we divide the time interval $(0, T)$ into N uniform subintervals by points $0 = t_0 < t_1 < \cdots < t_N = T$, where $t_k = k\tau$.

A fully explicit scheme can be formulated for (4.5): For any $1 \le n \le N-1$, find $\mathbf{E}_h^{n+1} \in \mathbf{V}_h$ such that

$$(\delta_\tau^2 \mathbf{E}_h^n, \mathbf{v}) + a_h(\mathbf{E}_h^n, \mathbf{v}) + \omega_p^2(\mathbf{E}_h^n, \mathbf{v}) - (\mathbf{J}_h^n, \mathbf{v}) = 0, \quad \forall \mathbf{v} \in \mathbf{V}_h, \tag{4.16}$$

subject to the initial approximation

$$\mathbf{E}_h^0 = \Pi_2 \mathbf{E}_0, \quad \mathbf{E}_h^1 = \Pi_2(\mathbf{E}_0 + \tau \mathbf{E}_1 + \frac{\tau^2}{2}\mathbf{E}_{tt}(0)), \tag{4.17}$$

where $\delta_\tau^2 \mathbf{E}_h^n = (\mathbf{E}_h^{n+1} - 2\mathbf{E}_h^n + \mathbf{E}_h^{n-1})/\tau^2$. Furthermore, $\mathbf{E}_{tt}(0) = -[\nabla \times (C_v^2 \nabla \times \mathbf{E}_0) + \omega_p^2 \mathbf{E}_0]$ is obtained by setting $t = 0$ in the governing equation (4.5), and $\mathbf{J}_h^n$ is obtained from the following recursive formula

$$\mathbf{J}_h^0 = 0, \quad \mathbf{J}_h^n = e^{-\nu\tau}\mathbf{J}_h^{n-1} + \frac{\nu\omega_p^2}{2}\tau(e^{-\nu\tau}\mathbf{E}_h^{n-1} + \mathbf{E}_h^n), \quad n \ge 1. \tag{4.18}$$

Theorem 4.2. *Let* $\mathbf{E}$ *and* $\mathbf{E}_h^n$ *be the solutions of the problem (4.5) and the finite element scheme (4.16)–(4.18) at time* t *and* t_n*, respectively. Under the CFL condition*

$$\tau < \frac{2h}{\sqrt{C_b + \omega_p^2 h^2}}, \tag{4.19}$$

where C_b *is the constant of Lemma 4.3. Furthermore, we assume that*

$$\mathbf{E}, \mathbf{E}_t \in L^\infty(0,T;(H^{\alpha+\sigma_E}(\Omega))^3), \quad \nabla \times \mathbf{E}, \nabla \times \mathbf{E}_t \in L^\infty(0,T;(H^\alpha(\Omega))^3),$$
$$\mathbf{E}_t, \mathbf{E}_{t^2}, \mathbf{E}_{t^3} \in L^\infty(0,T;(L^2(\Omega))^3), \quad \mathbf{E}_{t^4} \in L^2(0,T;(L^2(\Omega))^3).$$

Then there is a constant $C > 0$, independent of both the time step τ and mesh size h, such that

$$\max_{1\le n\le N} ||\mathbf{E}_h^n - \mathbf{E}^n||_0 \le C(\tau^2 + h^{\min(\alpha,l)+\sigma_E}), \quad l \ge 1,$$

where σ_E has the same meaning as in Theorem 4.1.

Interested readers can find the detailed proof in the original paper [186]. For smooth solutions on convex domain, we have the optimal L^2 error estimate:

$$\max_{1\le n\le N} ||\mathbf{E}_h^n - \mathbf{E}^n||_0 \le C(\tau^2 + h^{l+1}), \quad l \ge 1.$$

4.2.4 A Fully Implicit Scheme

An implicit scheme for (4.5) can be constructed as follows: For any $k \ge 1$, find $\mathbf{E}_h^{k+1} \in \mathbf{V}_h$ such that

$$(\delta_\tau^2 \mathbf{E}_h^k, v) + a_h(\overline{\mathbf{E}}_h^k v) + \omega_p^2(\overline{\mathbf{E}}_h^k, v) - (\mathbf{J}_h^k, v) = 0, \qquad \forall\, v \in \mathbf{V}_h, \tag{4.20}$$

subject to the same initial approximation $\mathbf{E}_h^0$ and $\mathbf{E}_h^1$ as (4.17), and the same recursive definition $\mathbf{J}_h^k$ as (4.18). Here we use the averaging operator $\overline{\mathbf{E}}_h^k = (\mathbf{E}_h^{k+1} + \mathbf{E}_h^{k-1})/2$.

Lemma 4.5. *For the $\mathbf{J}_h^k$ defined in (4.18), we have*

$$|\mathbf{J}_h^k| \le C\tau \sum_{j=0}^{k} |\mathbf{E}_h^j|, \quad \forall\, k \ge 1,$$

and

$$||\mathbf{J}_h^k||_0^2 \le CT\tau \sum_{j=0}^{k} ||\mathbf{E}_h^j||_0^2, \quad \forall\, k \ge 1.$$

Proof. Denote $a = e^{-\nu\tau}, b = \frac{\nu\omega_p^2}{2}\tau$. Then we can rewrite (4.18) as:

$$\mathbf{J}_h^k = a\mathbf{J}_h^{k-1} + ab\mathbf{E}_h^{k-1} + b\mathbf{E}_h^k,$$

from which we obtain

$$\begin{aligned}\mathbf{J}_h^k &= a(a\mathbf{J}_h^{k-2} + ab\mathbf{E}_h^{k-2} + b\mathbf{E}_h^{k-1}) + ab\mathbf{E}_h^{k-1} + b\mathbf{E}_h^k \\ &= a^2\mathbf{J}_h^{k-2} + a^2b\mathbf{E}_h^{k-2} + 2ab\mathbf{E}_h^{k-1} + b\mathbf{E}_h^k \\ &= a^2(a\mathbf{J}_h^{k-3} + ab\mathbf{E}_h^{k-3} + b\mathbf{E}_h^{k-2}) + a^2b\mathbf{E}_h^{k-2} + 2ab\mathbf{E}_h^{k-1} + b\mathbf{E}_h^k\end{aligned}$$

$$= a^3\mathbf{J}_h^{k-3} + a^3 b\mathbf{E}_h^{k-3} + 2a^2 b\mathbf{E}_h^{k-2} + 2ab\mathbf{E}_h^{k-1} + b\mathbf{E}_h^k$$
$$= \cdots$$
$$= a^k\mathbf{J}_h^0 + a^k b\mathbf{E}_h^0 + 2a^{k-1}b\mathbf{E}_h^1 + \cdots + 2a^2 b\mathbf{E}_h^{k-2} + 2ab\mathbf{E}_h^{k-1} + b\mathbf{E}_h^k. \quad (4.21)$$

Using $\mathbf{J}_h^0 = 0$ and the definitions of a and b in (4.21), we have

$$|\mathbf{J}_h^k| \le C\tau \sum_{j=0}^{k} |\mathbf{E}_h^j|,$$

which leads to

$$||\mathbf{J}_h^k||_0^2 \le C\tau^2 (\sum_{j=0}^{k} 1^2)(\sum_{j=0}^{k} ||\mathbf{E}_h^j||_0^2) \le CT\tau \sum_{j=0}^{k} ||\mathbf{E}_h^j||_0^2,$$

which concludes the proof. □

Using Lemma 4.5, we can prove the following unconditional stability for the scheme (4.20).

Theorem 4.3. *Denote the backward difference* $\partial_\tau u^k = (u^k - u^{k-1})/\tau$. *Then for the solution of scheme (4.20), we have*

$$||\partial_\tau \mathbf{E}_h^n||_0^2 + ||\mathbf{E}_h^n||_h^2 \le C(||\mathbf{E}_h^1||_h^2 + ||\mathbf{E}_h^0||_h^2 + ||\partial_\tau \mathbf{E}_h^1||_0^2), \quad \forall n \ge 2.$$

Proof. Choosing $v = \mathbf{E}_h^{k+1} - \mathbf{E}_h^{k-1} = \tau(\partial_\tau \mathbf{E}_h^{k+1} + \partial_\tau \mathbf{E}_h^k)$ in (4.20), we obtain

$$||\partial_\tau \mathbf{E}_h^{k+1}||_0^2 - ||\partial_\tau \mathbf{E}_h^k||_0^2 + \frac{1}{2}(\widetilde{a}_h(\mathbf{E}_h^{k+1}, \mathbf{E}_h^{k+1}) - \widetilde{a}_h(\mathbf{E}_h^{k-1}, \mathbf{E}_h^{k-1}))$$
$$+ \frac{\omega_p^2}{2}(||\mathbf{E}_h^{k+1}||_0^2 - ||\mathbf{E}_h^{k-1}||_0^2) = \tau(\mathbf{J}_h^k, \partial_\tau \mathbf{E}_h^{k+1} + \partial_\tau \mathbf{E}_h^k). \quad (4.22)$$

Summing up (4.22) from $k = 1$ to $k = n-1$ $(2 \le n \le M)$, we have

$$||\partial_\tau \mathbf{E}_h^n||_0^2 - ||\partial_\tau \mathbf{E}_h^1||_0^2 + \frac{1}{2}(\widetilde{a}_h(\mathbf{E}_h^n, \mathbf{E}_h^n) + \widetilde{a}_h(\mathbf{E}_h^{n-1}, \mathbf{E}_h^{n-1}) - \widetilde{a}_h(\mathbf{E}_h^1, \mathbf{E}_h^1) - \widetilde{a}_h(\mathbf{E}_h^0, \mathbf{E}_h^0))$$
$$+ \frac{\omega_p^2}{2}(||\mathbf{E}_h^n||_0^2 + ||\mathbf{E}_h^{n-1}||_0^2 - ||\mathbf{E}_h^1||_0^2 - ||\mathbf{E}_h^0||_0^2)$$
$$= \tau \sum_{k=1}^{n-1} (\mathbf{J}_h^k, \partial_\tau \mathbf{E}_h^{k+1} + \partial_\tau \mathbf{E}_h^k). \quad (4.23)$$

By Lemma 4.5, we obtain

$$\begin{aligned}
&\tau \sum_{k=1}^{n-1} (\mathbf{J}_h^k, \partial_\tau \mathbf{E}_h^{k+1} + \partial_\tau \mathbf{E}_h^k) \\
&\leq \tau \sum_{k=1}^{n-1} \left(\frac{1}{2\delta_1} ||\mathbf{J}_h^k||_0^2 + \frac{\delta_1}{2} ||\partial_\tau \mathbf{E}_h^{k+1} + \partial_\tau \mathbf{E}_h^k||_0^2\right) \\
&\leq \frac{\tau}{2\delta_1} \sum_{k=1}^{n-1} \left(CT\tau \sum_{j=0}^{k} ||\mathbf{E}_h^j||_0^2\right) + \delta_1 \tau \sum_{k=1}^{n-1} \left(||\partial_\tau \mathbf{E}_h^{k+1}||_0^2 + ||\partial_\tau \mathbf{E}_h^k||_0^2\right) \\
&\leq CT^2 \tau \sum_{k=0}^{n-1} ||\mathbf{E}_h^k||_0^2 + 2\delta_1 \tau \sum_{k=1}^{n-1} ||\partial_\tau \mathbf{E}_h^k||_0^2 + \delta_1 \tau ||\partial_\tau \mathbf{E}_h^n||_0^2. \qquad (4.24)
\end{aligned}$$

Substituting (4.24) into (4.23), choosing δ_1 small enough, then using the discrete Gronwall inequality, we obtain

$$||\partial_\tau \mathbf{E}_h^n||_0^2 + ||\mathbf{E}_h^n||_h^2 \leq C(||\mathbf{E}_h^1||_h^2 + ||\mathbf{E}_h^0||_h^2 + ||\partial_\tau \mathbf{E}_h^1||_0^2),$$

which concludes the proof. □

The following optimal error estimate is proved in [155].

Theorem 4.4. *Let* $\mathbf{E}$ *and* $\mathbf{E}_h^k$ *be the solutions of the problem (4.5) and the finite element scheme (4.20) at the time* t *and* t_k*, respectively. Under the regularity assumptions:*

$$\begin{aligned}
&\mathbf{E}, \nabla \times \mathbf{E} \in L^\infty(0, T; (H^{\alpha+\sigma_E}(\Omega))^3), \quad \nabla \times \mathbf{E}_{tt} \in L^2(0, T; (H^\alpha(\Omega))^3), \\
&\mathbf{E}_t, \mathbf{E}_{tt}, \nabla \times \nabla \times \mathbf{E}_{tt} \in L^2(0, T; (L^2(\Omega))^3), \\
&\mathbf{E}_{t^3} \in L^\infty(0, \tau; H(curl; \Omega)), \ \nabla \times \mathbf{E}_{t^3} \in L^\infty(0, \tau; (H^\alpha(\Omega))^3),
\end{aligned}$$

there is a constant $C > 0$*, independent of time step* τ *and mesh size* h*, such that*

$$\max_{1 \leq n \leq M} ||\mathbf{E}_h^n - \mathbf{E}^n||_0 \leq C(\tau^2 + h^{\min(\alpha, l)+\sigma_E}),$$

and

$$\max_{1 \leq n \leq M} ||\mathbf{E}_h^n - \mathbf{E}^n||_h \leq C(\tau^2 + h^{\min(\alpha, l)}),$$

where $l \geq 1$ *is the degree of the polynomial function in the finite element space (4.11). Hence, on a convex domain* Ω*, if the solution* $\mathbf{E}$ *has enough regularity, we have the optimal error estimates*

$$\max_{1 \leq n \leq M} ||\mathbf{E}_h^n - \mathbf{E}^n||_0 \leq C(\tau^2 + h^{l+1}), \quad \max_{1 \leq n \leq M} |\mathbf{E}_h^n - \mathbf{E}^n|_h \leq C(\tau^2 + h^l).$$

4.3 Discontinuous Galerkin Methods for the Drude Model

Taking the product of Eqs. (1.18)–(1.21) by test functions $\mathbf{u}, \mathbf{v}, \boldsymbol{\phi}, \boldsymbol{\psi}$ and integrating by parts over any element $T_i \in T_h$, we have

$$\epsilon_0 \int_{T_i} \frac{\partial \mathbf{E}}{\partial t} \cdot \mathbf{u} - \int_{T_i} \mathbf{H} \cdot \nabla \times \mathbf{u} - \int_{\partial T_i} \mathbf{n}_i \times \mathbf{H} \cdot \mathbf{u} + \int_{T_i} \mathbf{J} \cdot \mathbf{u} = 0, \tag{4.25}$$

$$\mu_0 \int_{T_i} \frac{\partial \mathbf{H}}{\partial t} \cdot \mathbf{v} + \int_{T_i} \mathbf{E} \cdot \nabla \times \mathbf{v} + \int_{\partial T_i} \mathbf{n}_i \times \mathbf{E} \cdot \mathbf{v} + \int_{T_i} \mathbf{K} \cdot \mathbf{v} = 0, \tag{4.26}$$

$$\frac{1}{\epsilon_0 \omega_{pe}^2} \int_{T_i} \frac{\partial \mathbf{J}}{\partial t} \cdot \phi + \frac{\Gamma_e}{\epsilon_0 \omega_{pe}^2} \int_{T_i} \mathbf{J} \cdot \phi = \int_{T_i} \mathbf{E} \cdot \phi, \tag{4.27}$$

$$\frac{1}{\mu_0 \omega_{pm}^2} \int_{T_i} \frac{\partial \mathbf{K}}{\partial t} \cdot \psi + \frac{\Gamma_m}{\mu_0 \omega_{pm}^2} \int_{T_i} \mathbf{K} \cdot \psi = \int_{T_i} \mathbf{H} \cdot \psi. \tag{4.28}$$

Let us look at the semi-discrete solution $\mathbf{E}_h, \mathbf{H}_h, \mathbf{J}_h, \mathbf{K}_h \in C^1(0, T; \mathbf{V}_h)$ as a solution of the following weak formulation: For any $\mathbf{u}_h, \mathbf{v}_h, \phi_h, \psi_h \in \mathbf{V}_h$, and any element $T_i \in T_h$,

$$\epsilon_0 \int_{T_i} \frac{\partial \mathbf{E}_h}{\partial t} \cdot \mathbf{u}_h - \int_{T_i} \mathbf{H}_h \cdot \nabla \times \mathbf{u}_h - \sum_{K \in \nu_i} \int_{a_{ik}} \mathbf{u}_h \cdot \mathbf{n}_{ik} \times \{\{\mathbf{H}_h\}\}_{ik} + \int_{T_i} \mathbf{J}_h \cdot \mathbf{u}_h = 0, \tag{4.29}$$

$$\mu_0 \int_{T_i} \frac{\partial \mathbf{H}_h}{\partial t} \cdot \mathbf{v}_h + \int_{T_i} \mathbf{E}_h \cdot \nabla \times \mathbf{v}_h + \sum_{K \in \nu_i} \int_{a_{ik}} \mathbf{v}_h \cdot \mathbf{n}_{ik} \times \{\{\mathbf{E}_h\}\}_{ik} + \int_{T_i} \mathbf{K}_h \cdot \mathbf{v}_h = 0, \tag{4.30}$$

$$\frac{1}{\epsilon_0 \omega_{pe}^2} \int_{T_i} \frac{\partial \mathbf{J}_h}{\partial t} \cdot \phi_h + \frac{\Gamma_e}{\epsilon_0 \omega_{pe}^2} \int_{T_i} \mathbf{J}_h \cdot \phi_h = \int_{T_i} \mathbf{E}_h \cdot \phi_h, \tag{4.31}$$

$$\frac{1}{\mu_0 \omega_{pm}^2} \int_{T_i} \frac{\partial \mathbf{K}_h}{\partial t} \cdot \psi_h + \frac{\Gamma_m}{\mu_0 \omega_{pm}^2} \int_{T_i} \mathbf{K}_h \cdot \psi_h = \int_{T_i} \mathbf{H}_h \cdot \psi_h, \tag{4.32}$$

hold true and are subject to the initial conditions:

$$\mathbf{E}_h(0) = \Pi_2 \mathbf{E}_0,\ \mathbf{H}_h(0) = \Pi_2 \mathbf{H}_0,\ \mathbf{J}_h(0) = \Pi_2 \mathbf{J}_0,\ \mathbf{K}_h(0) = \Pi_2 \mathbf{K}_0, \tag{4.33}$$

where Π_2 denotes the standard L^2-projection onto $\mathbf{V}_h$. Recall that $\mathbf{E}_0, \mathbf{H}_0, \mathbf{J}_0$ and $\mathbf{K}_0$ are the given initial condition functions. Here we denote V_i for the set of indices of all neighboring elements of T_i and a_{ik} for the internal face $a_{ik} = T_i \cap T_k$.

Denote the semi-discrete energy $\mathscr{E}_h$:

$$\mathscr{E}_h(t) = \frac{1}{2}(\epsilon_0 ||\mathbf{E}_h(t)||_0^2 + \mu_0 ||\mathbf{H}_h(t)||_0^2 + \frac{1}{\epsilon_0 \omega_{pe}^2} ||\mathbf{J}_h(t)||_0^2 + \frac{1}{\mu_0 \omega_{pm}^2} ||\mathbf{K}_h(t)||_0^2), \tag{4.34}$$

and a bilinear form $\mathscr{B}_i$:

$$\mathscr{B}_i(\mathbf{E},\mathbf{H}) = -\int_{T_i} \mathbf{H}_i \cdot \nabla \times \mathbf{E}_i - \sum_{K\in v_i} \int_{a_{ik}} \mathbf{E}_h \cdot \mathbf{n}_{ik} \times \{\{\mathbf{H}_h\}\}_{ik} + \int_{T_i} \mathbf{E}_i \cdot \nabla \times \mathbf{H}_i + \sum_{K\in v_i} \int_{a_{ik}} \mathbf{H}_h \cdot \mathbf{n}_{ik} \times \{\{\mathbf{E}_h\}\}_{ik}. \tag{4.35}$$

Theorem 4.5. *The energy $\mathscr{E}_h$ is decreasing in time, i.e., $\mathscr{E}_h(t) \le \mathscr{E}_h(0)$.*

Proof. Choosing $\mathbf{u}_h = \mathbf{E}_h, \mathbf{v}_h = \mathbf{H}_h, \phi_h = \mathbf{J}_h, \psi_h = \mathbf{K}_h$ in (4.29)–(4.32) and adding the results together over all element $T_i \in T_h$, we obtain

$$\frac{d}{dt}\mathscr{E}_h(t) + \frac{\Gamma_e}{\epsilon_0\omega_{pe}^2}||\mathbf{J}_h(t)||_0^2 + \frac{\Gamma_m}{\mu_0\omega_{pm}^2}||\mathbf{K}_h(t)||_0^2 + \sum_i \mathscr{B}_i(\mathbf{E},\mathbf{H}) = 0. \tag{4.36}$$

By the definition of $\mathscr{B}_i$ and integration by parts, we have

$$\begin{aligned}\mathscr{B}_i(\mathbf{E},\mathbf{H}) &= \sum_{K\in v_i} \int_{a_{ik}} \mathbf{E}_i \cdot \mathbf{n}_{ik} \times \mathbf{H}_i \\ &\quad + \sum_{K\in v_i} \int_{a_{ik}} \mathbf{E}_i \cdot \{\{\mathbf{H}_h\}\}_{ik} \times \mathbf{n}_{ik} - \sum_{K\in v_i} \int_{a_{ik}} \mathbf{H}_i \cdot \{\{\mathbf{E}_h\}\}_{ik} \times \mathbf{n}_{ik} \\ &= \sum_{K\in v_i} \int_{a_{ik}} [-\mathbf{E}_i \times \mathbf{H}_i + \mathbf{E}_i \times \frac{\mathbf{H}_i + \mathbf{H}_k}{2} - \mathbf{H}_i \times \frac{\mathbf{E}_i + \mathbf{E}_k}{2}] \cdot \mathbf{n}_{ik} \\ &= \frac{1}{2} \sum_{K\in v_i} \int_{a_{ik}} (\mathbf{E}_i \times \mathbf{H}_k + \mathbf{E}_k \times \mathbf{H}_i) \cdot \mathbf{n}_{ik}. \end{aligned} \tag{4.37}$$

From (4.37), we obtain $\sum_i \mathscr{B}_i(\mathbf{E},\mathbf{H}) = 0$, which, along with (4.36), concludes the proof. □

For the semi-discrete scheme (4.29)–(4.32), we have the following convergence result.

Theorem 4.6. *If $\mathbf{E},\mathbf{H},\mathbf{J},\mathbf{K} \in C^0([0,T];(H^{s+1}(\Omega))^3)$ for $s \ge 0$, then there exists a constant $C > 0$ independent of h such that*

$$\begin{aligned}&\max_{t\in[0,T]} (||\mathbf{E}-\mathbf{E}_h||_0 + ||\mathbf{H}-\mathbf{H}_h||_0 + ||\mathbf{J}-\mathbf{J}_h||_0 + ||\mathbf{K}-\mathbf{K}_h||_0) \\ &\le C h^{\min(s,k)} ||(\mathbf{E},\mathbf{H},\mathbf{J},\mathbf{K})||_{C^0([0,T];(H^{s+1}(\Omega))^3)}. \end{aligned} \tag{4.38}$$

Proof. Let us introduce the notation $\tilde{\mathbf{W}}_h = \Pi_2(\mathbf{W}) - \mathbf{W}_h$ and $\overline{\mathbf{W}}_h = \Pi_2(\mathbf{W}) - \mathbf{W}$ for $\mathbf{W} = \mathbf{E},\mathbf{H},\mathbf{J},\mathbf{K}$.

Subtracting (4.29)–(4.32) from (4.25)–(4.28), we have the error equations:

$$(i)\ \epsilon_0 \int_{T_i} \frac{\partial \tilde{\mathbf{E}}_h}{\partial t} \cdot \mathbf{u}_h - \int_{T_i} \tilde{\mathbf{H}}_h \cdot \nabla \times \mathbf{u}_h - \sum_{K \in \nu_i} \int_{a_{ik}} \mathbf{u}_h \cdot \mathbf{n}_{ik} \times \{\{\tilde{\mathbf{H}}_h\}\}_{ik} + \int_{T_i} \tilde{\mathbf{J}}_h \cdot \mathbf{u}_h$$
$$= \epsilon_0 \int_{T_i} \frac{\partial \overline{\mathbf{E}}_h}{\partial t} \cdot \mathbf{u}_h - \int_{T_i} \overline{\mathbf{H}}_h \cdot \nabla \times \mathbf{u}_h - \sum_{K \in \nu_i} \int_{a_{ik}} \mathbf{u}_h \cdot \mathbf{n}_{ik} \times \{\{\overline{\mathbf{H}}_h\}\}_{ik} + \int_{T_i} \overline{\mathbf{J}}_h \cdot \mathbf{u}_h, \tag{4.39}$$

$$(ii)\ \mu_0 \int_{T_i} \frac{\partial \tilde{\mathbf{H}}_h}{\partial t} \cdot \mathbf{v}_h + \int_{T_i} \tilde{\mathbf{E}}_h \cdot \nabla \times \mathbf{v}_h + \sum_{K \in \nu_i} \int_{a_{ik}} \mathbf{v}_h \cdot \mathbf{n}_{ik} \times \{\{\tilde{\mathbf{E}}_h\}\}_{ik} + \int_{T_i} \tilde{\mathbf{K}}_h \cdot \mathbf{v}_h$$
$$= \mu_0 \int_{T_i} \frac{\partial \overline{\mathbf{H}}_h}{\partial t} \cdot \mathbf{v}_h + \int_{T_i} \overline{\mathbf{E}}_h \cdot \nabla \times \mathbf{v}_h + \sum_{K \in \nu_i} \int_{a_{ik}} \mathbf{v}_h \cdot \mathbf{n}_{ik} \times \{\{\overline{\mathbf{E}}_h\}\}_{ik} + \int_{T_i} \overline{\mathbf{K}}_h \cdot \mathbf{v}_h, \tag{4.40}$$

$$(iii)\ \frac{1}{\epsilon_0 \omega_{pe}^2} \int_{T_i} \frac{\partial \tilde{\mathbf{J}}_h}{\partial t} \cdot \phi_h + \frac{\Gamma_e}{\epsilon_0 \omega_{pe}^2} \int_{T_i} \tilde{\mathbf{J}}_h \cdot \phi_h - \int_{T_i} \tilde{\mathbf{E}}_h \cdot \phi_h$$
$$= \frac{1}{\epsilon_0 \omega_{pe}^2} \int_{T_i} \frac{\partial \overline{\mathbf{J}}_h}{\partial t} \cdot \phi_h + \frac{\Gamma_e}{\epsilon_0 \omega_{pe}^2} \int_{T_i} \overline{\mathbf{J}}_h \cdot \phi_h - \int_{T_i} \overline{\mathbf{E}}_h \cdot \phi_h, \tag{4.41}$$

$$(iv)\ \frac{1}{\mu_0 \omega_{pm}^2} \int_{T_i} \frac{\partial \tilde{\mathbf{K}}_h}{\partial t} \cdot \psi_h + \frac{\Gamma_m}{\mu_0 \omega_{pm}^2} \int_{T_i} \tilde{\mathbf{K}}_h \cdot \psi_h - \int_{T_i} \tilde{\mathbf{H}}_h \cdot \psi_h$$
$$= \frac{1}{\mu_0 \omega_{pm}^2} \int_{T_i} \frac{\partial \overline{\mathbf{K}}_h}{\partial t} \cdot \psi_h + \frac{\Gamma_m}{\mu_0 \omega_{pm}^2} \int_{T_i} \overline{\mathbf{K}}_h \cdot \psi_h - \int_{T_i} \overline{\mathbf{H}}_h \cdot \psi_h. \tag{4.42}$$

Choosing $\mathbf{u}_h = \tilde{\mathbf{E}}_h, \mathbf{v}_h = \tilde{\mathbf{H}}_h, \phi_h = \tilde{\mathbf{J}}_h, \psi_h = \tilde{\mathbf{K}}_h$ in (4.39)–(4.42), summing up the results for all elements T_i of T_h, then using the projection property and the energy definition (4.34), we have

$$\frac{d}{dt}\tilde{\mathscr{E}}_h + \frac{\Gamma_e}{\epsilon_0 \omega_{pe}^2} ||\tilde{\mathbf{J}}_h||_0^2 + \frac{\Gamma_m}{\mu_0 \omega_{pm}^2} ||\tilde{\mathbf{K}}_h||_0^2 + \sum_i \mathscr{B}_i(\tilde{\mathbf{E}}, \tilde{\mathbf{H}})$$
$$= \sum_i \sum_{K \in \nu_i} [\int_{a_{ik}} \tilde{\mathbf{E}}_h \cdot \mathbf{n}_{ik} \times \{\{\overline{\mathbf{H}}_h\}\}_{ik} + \int_{a_{ik}} \tilde{\mathbf{H}}_h \cdot \mathbf{n}_{ik} \times \{\{\overline{\mathbf{E}}_h\}\}_{ik}]$$
$$\leq \sum_i [||\tilde{\mathbf{E}}_h||_{0,\partial T_i} ||\overline{\mathbf{H}}_h||_{0,\partial T_i} + ||\tilde{\mathbf{H}}_h||_{0,\partial T_i} ||\overline{\mathbf{E}}_h||_{0,\partial T_i}]$$
$$\leq \sum_i [C h_{T_i}^{-\frac{1}{2}} ||\tilde{\mathbf{E}}_h||_{0,T_i} C h_{T_i}^{\min(s,k)+\frac{1}{2}} ||\mathbf{H}||_{s+1,T_i} + C h_{T_i}^{-\frac{1}{2}} ||\tilde{\mathbf{H}}_h||_{0,T_i} C h_{T_i}^{\min(s,k)+\frac{1}{2}} ||\mathbf{E}||_{s+1,T_i}],$$

where in the last step we used the standard inverse inequality and interpolation error estimate.

The proof is completed by using the fact $\sum_i \mathscr{B}_i(\tilde{\mathbf{E}}, \tilde{\mathbf{H}}) = 0$ and the Gronwall inequality. □

Similar to those fully-discrete schemes developed in Chap. 3, we can construct a simple leap-frog scheme as follows: find $\mathbf{E}_h^{n+1}, \mathbf{H}_h^{n+\frac{3}{2}}, \mathbf{J}_h^{n+\frac{3}{2}}, \mathbf{K}_h^{n+1} \in \mathbf{V}_h$ such that for any $\mathbf{u}_h, \mathbf{v}_h, \phi_h, \psi_h \in \mathbf{V}_h$, and any element $T_i \in T_h$,

$$
\begin{aligned}
&\epsilon_0 \int_{T_i} \frac{\mathbf{E}_i^{n+1} - \mathbf{E}_i^n}{\tau} \cdot \mathbf{u}_h - \int_{T_i} \mathbf{H}_i^{n+\frac{1}{2}} \cdot \nabla \times \mathbf{u}_h \\
&\quad - \sum_{K \in v_i} \int_{a_{ik}} \mathbf{u}_h \cdot \mathbf{n}_{ik} \times \{\{\mathbf{H}_h^{n+\frac{1}{2}}\}\}_{ik} + \int_{T_i} \mathbf{J}_i^{n+\frac{1}{2}} \cdot \mathbf{u}_h = 0, \\
&\mu_0 \int_{T_i} \frac{\mathbf{H}_h^{n+\frac{3}{2}} - \mathbf{H}_h^{n+\frac{1}{2}}}{\tau} \cdot \mathbf{v}_h + \int_{T_i} \mathbf{E}_i^{n+1} \cdot \nabla \times \mathbf{v}_h \\
&\quad + \sum_{K \in v_i} \int_{a_{ik}} \mathbf{v}_h \cdot \mathbf{n}_{ik} \times \{\{\mathbf{E}_h^{n+1}\}\}_{ik} + \int_{T_i} \mathbf{K}_i^{n+1} \cdot \mathbf{v}_h = 0, \\
&\frac{1}{\epsilon_0 \omega_{pe}^2} \int_{T_i} \frac{\mathbf{J}_i^{n+\frac{3}{2}} - \mathbf{J}_i^{n+\frac{1}{2}}}{\tau} \cdot \phi_h + \frac{\Gamma_e}{\epsilon_0 \omega_{pe}^2} \int_{T_i} \frac{\mathbf{J}_i^{n+\frac{3}{2}} + \mathbf{J}_i^{n+\frac{1}{2}}}{2} \cdot \phi_h = \int_{T_i} \mathbf{E}_i^{n+1} \cdot \phi_h, \\
&\frac{1}{\mu_0 \omega_{pm}^2} \int_{T_i} \frac{\mathbf{K}_i^{n+1} - \mathbf{K}_i^n}{\tau} \cdot \psi_h + \frac{\Gamma_m}{\mu_0 \omega_{pm}^2} \int_{T_i} \frac{\mathbf{K}_i^{n+1} + \mathbf{K}_i^n}{2} \cdot \psi_h = \int_{T_i} \mathbf{H}_i^{n+\frac{1}{2}} \cdot \psi_h,
\end{aligned}
$$

subject to the initial conditions (4.33). Stability and convergence analysis can be carried out for this scheme. We leave the details to interested readers.

4.4 Nodal Discontinuous Galerkin Methods for the Drude Model

In this section, we extend the nodal discontinuous Galerkin methods developed by Hesthaven and Warburton [141] for general conservation laws to solve Maxwell's equations when metamaterials are involved. The package *nudg* developed in [141] provides a very good template for solving many common partial differential equations such as elliptic problems, Euler equations, Maxwell's equations and Navier-Stokes equations. Here we provide detailed MATLAB source codes to show readers how to modify the package *nudg* to solve the metamaterial Maxwell's equations. The contents of this section are mainly derived from Li [185].

4.4.1 The Algorithm

To simplify the presentation, we first non-dimensionalize the Drude model equations (1.18)–(1.21). Let us introduce the vacuum speed of light C_v, the vacuum impedance Z_0:

$$C_v = \frac{1}{\sqrt{\epsilon_0 \mu_0}} \approx 3 \times 10^8 \text{ m/s}, \quad Z_0 = \sqrt{\mu_0/\epsilon_0} \approx 120\pi \text{ ohms},$$

and unit-free variables

$$\tilde{t} = \frac{C_v t}{L}, \quad \tilde{x} = \frac{x}{L},$$
$$\tilde{\Gamma}_e = \frac{\Gamma_e L}{C_v}, \quad \tilde{\omega}_{pe} = \frac{\omega_{pe} L}{C_v}, \quad \tilde{\Gamma}_m = \frac{\Gamma_m L}{C_v}, \quad \tilde{\omega}_{pm} = \frac{\omega_{pm} L}{C_v},$$
$$\tilde{\mathbf{E}} = \frac{\mathbf{E}}{Z_0 H_0}, \quad \tilde{\mathbf{H}} = \frac{\mathbf{H}}{H_0}, \quad \tilde{\mathbf{J}} = \frac{L\mathbf{J}}{H_0}, \quad \tilde{\mathbf{K}} = \frac{L\mathbf{K}}{Z_0 H_0},$$

where H_0 is a unit magnetic field strength, and L is a reference length (typically the wavelength of one interested object).

It is not difficult to check that the equations (1.18)–(1.21) can be written as

$$\frac{\partial \tilde{\mathbf{E}}}{\partial \tilde{t}} = \nabla \times \tilde{\mathbf{H}} - \tilde{\mathbf{J}}, \tag{4.43}$$

$$\frac{\partial \tilde{\mathbf{H}}}{\partial \tilde{t}} = -\nabla \times \tilde{\mathbf{E}} - \tilde{\mathbf{K}}, \tag{4.44}$$

$$\frac{\partial \tilde{\mathbf{J}}}{\partial \tilde{t}} + \tilde{\Gamma}_e \tilde{\mathbf{J}} = \tilde{\omega}_e^2 \tilde{\mathbf{E}}, \tag{4.45}$$

$$\frac{\partial \tilde{\mathbf{K}}}{\partial \tilde{t}} + \tilde{\Gamma}_m \tilde{\mathbf{K}} = \tilde{\omega}_m^2 \tilde{\mathbf{H}}, \tag{4.46}$$

which have the same form as the original governing equations (1.18)–(1.21) if we set $\epsilon_0 = \mu_0 = 1$ in (1.18)–(1.21).

In the rest of this section, our discussion is based on the non-dimensionalized form (4.43)–(4.46) by dropping all those tildes and adding fixed sources $\mathbf{f}$ and $\mathbf{g}$ to (4.43) and (4.44), i.e.,

$$\frac{\partial \mathbf{E}}{\partial t} = \nabla \times \mathbf{H} - \mathbf{J} + \mathbf{f}, \tag{4.47}$$

$$\frac{\partial \mathbf{H}}{\partial \tilde{t}} = -\nabla \times \mathbf{E} - \mathbf{K} + \mathbf{g}, \tag{4.48}$$

$$\frac{\partial \mathbf{J}}{\partial t} + \Gamma_e \mathbf{J} = \omega_e^2 \mathbf{E}, \tag{4.49}$$

$$\frac{\partial \mathbf{K}}{\partial t} + \Gamma_m \mathbf{K} = \omega_m^2 \mathbf{H}, \tag{4.50}$$

Using the same idea as [140], we can rewrite (4.47) and (4.48) in the conservation form

$$\frac{\partial \mathbf{q}}{\partial t} + \nabla \cdot \psi(\mathbf{q}) = \mathbf{S}, \tag{4.51}$$

where we denote

$$\mathbf{q} = \begin{bmatrix} \mathbf{E} \\ \mathbf{H} \end{bmatrix}, \quad \mathbf{S} \equiv \begin{bmatrix} S_E \\ S_H \end{bmatrix} = \begin{bmatrix} -\mathbf{J} + \mathbf{f} \\ -\mathbf{K} + \mathbf{g} \end{bmatrix}, \quad F_i(\mathbf{q}) = \begin{bmatrix} -\mathbf{e}_i \times \mathbf{H} \\ \mathbf{e}_i \times \mathbf{E} \end{bmatrix},$$

and $\psi(\mathbf{q}) = [F_1(\mathbf{q}), F_2(\mathbf{q}), F_3(\mathbf{q})]^T$. Here $\mathbf{e}_i$ are the three Cartesian unit vectors.

We assume that the domain Ω is decomposed into tetrahedral (or triangular in 2-D) elements Ω_k, and the numerical solution $\mathbf{q}_N$ is represented as

$$\mathbf{q}_N(\mathbf{x}, t) = \sum_{j=1}^{N_n} \mathbf{q}_j(\mathbf{x}_j, t) L_j(\mathbf{x}) = \sum_{j=1}^{N_n} \mathbf{q}_j(t) L_j(\mathbf{x}), \tag{4.52}$$

where $L_j(\mathbf{x})$ is the multivariate Lagrange interpolation polynomial of degree n. Here $N_n = \frac{1}{6}(n+1)(n+2)(n+3)$ in 3-D; while $N_n = \frac{1}{2}(n+1)(n+2)$ in 2-D.

Multiplying (4.51) by a test function $L_i(\mathbf{x})$ and integrating over each element Ω_k, we obtain

$$\int_{\Omega_k} \left(\frac{\partial \mathbf{q}_N}{\partial t} + \nabla \cdot \psi(\mathbf{q}_N) - \mathbf{S}_N\right) L_i(\mathbf{x}) dx = \int_{\partial \Omega_k} \hat{\mathbf{n}} \cdot (\psi(\mathbf{q}_N) - \psi_N^*) L_i(\mathbf{x}) dx, \tag{4.53}$$

where $\hat{\mathbf{n}}$ is an outward normal unit vector of $\partial \Omega_k$, and ψ_N^* is a numerical flux. For the Maxwell's equations, we usually choose the upwind flux [140]

$$\hat{\mathbf{n}} \cdot (\psi(\mathbf{q}_N) - \psi_N^*) = \begin{cases} \frac{1}{2}\hat{\mathbf{n}} \times ([\mathbf{H}_N] - \hat{\mathbf{n}} \times [\mathbf{E}_N]) \\ \frac{1}{2}\hat{\mathbf{n}} \times (-\hat{\mathbf{n}} \times [\mathbf{H}_N] - [\mathbf{E}_N]) \end{cases},$$

where $[\mathbf{E}_N] = \mathbf{E}_N^+ - \mathbf{E}_N^-$, and $[\mathbf{H}_N] = \mathbf{H}_N^+ - \mathbf{H}_N^-$. Here superscripts '+' and '−' refer to field values from the neighboring element and the local element, respectively.

Substituting (4.52) into (4.53), we obtain the elementwise equations for the electric field components

$$\sum_{j=0}^{N} \left(M_{ij} \frac{d\mathbf{E}_j}{dt} - S_{ij} \times \mathbf{H}_j - M_{ij} \mathbf{S}_{E,j}\right) = \frac{1}{2} \sum_l F_{il} \cdot \hat{\mathbf{n}}_l \times ([\mathbf{H}_l] - \hat{\mathbf{n}}_l \times [\mathbf{E}_l]), \tag{4.54}$$

and for the magnetic field components

$$\sum_{j=0}^{N}(M_{ij}\frac{d\mathbf{H}_j}{dt}+S_{ij}\times\mathbf{E}_j-M_{ij}\mathbf{S}_{H,j})=\frac{1}{2}\sum_l F_{il}\cdot\hat{\mathbf{n}}_l\times(-\hat{\mathbf{n}}_l\times[\mathbf{H}_l]-[\mathbf{E}_l]),\quad(4.55)$$

where

$$M_{ij}=(L_i(\mathbf{x}),L_j(\mathbf{x}))_{\Omega_k},\quad S_{ij}=(L_i(\mathbf{x}),\nabla L_j(\mathbf{x}))_{\Omega_k}$$

represent the local mass and stiffness matrices, respectively. Furthermore,

$$F_{il}=(L_i(\mathbf{x}),L_l(\mathbf{x}))_{\partial\Omega_k}$$

represents the face-based mass matrix.

We can rewrite (4.54) and (4.55) in a fully explicit form, while the constitutive equations (4.49) and (4.50) keep the same form. In summary, we have the following semi-discrete discontinuous Galerkin scheme:

$$\frac{d\mathbf{E}_N}{dt}=M^{-1}S\times\mathbf{H}_N-\mathbf{J}_N+\mathbf{f}_N+\frac{1}{2}M^{-1}F\Big(\hat{\mathbf{n}}\times([\mathbf{H}_N]-\hat{\mathbf{n}}\times[\mathbf{E}_N])\Big)|_{\partial\Omega_k},\quad(4.56)$$

$$\frac{d\mathbf{H}_N}{dt}=-M^{-1}S\times\mathbf{E}_N-\mathbf{K}_N+\mathbf{g}_N-\frac{1}{2}M^{-1}F\Big(\hat{\mathbf{n}}\times(\hat{\mathbf{n}}\times[\mathbf{H}_N]+[\mathbf{E}_N])\Big)|_{\partial\Omega_k},$$

$$\frac{d\mathbf{J}_N}{dt}=\omega_e^2\mathbf{E}_N-\Gamma_e\mathbf{J}_N,\quad(4.57)$$

$$\frac{d\mathbf{K}_N}{dt}=\omega_m^2\mathbf{H}_N-\Gamma_m\mathbf{K}_N.\quad(4.58)$$

The system (4.56)–(4.58) can be solved by various methods used for ordinary differential equations. Below we adopt the classic low-storage five-stage fourth-order explicit Runge-Kutta method [141, Sect. 3.4].

4.4.2 MATLAB Codes and Numerical Results

We implement the above algorithm using the package *nudg* provided by Hesthaven and Warburton [141]. Considering that the 3-D case is quite similar to the 2-D case (though computational time in 3-D is much longer), here we only consider the 2-D transverse magnetic mode with respect to z (TM_z: no magnetic field in z-direction) metamaterial model:

$$\frac{\partial H_x}{\partial t}=-\frac{\partial E_z}{\partial y}-K_x+g_x\quad(4.59)$$

$$\frac{\partial H_y}{\partial t}=\frac{\partial E_z}{\partial x}-K_y+g_y\quad(4.60)$$

$$\frac{\partial E_z}{\partial t} = \frac{\partial H_y}{\partial x} - \frac{\partial H_x}{\partial y} - J_z + f \tag{4.61}$$

$$\frac{\partial J_z}{\partial t} = \omega_e^2 E_z - \Gamma_e J_z \tag{4.62}$$

$$\frac{\partial K_x}{\partial t} = \omega_m^2 H_x - \Gamma_m K_x \tag{4.63}$$

$$\frac{\partial K_y}{\partial t} = \omega_m^2 H_y - \Gamma_m K_y \tag{4.64}$$

where the subscripts 'x, y' and 'z' denote the corresponding components.

For the metamaterial model (4.59)–(4.64), we only need to provide three main MATLAB functions: *Meta2DDriver.m*, *MetaRHS2D.m*, and *Meta2D.m*. The rest supporting functions are provided by the package *nudg* of Hesthaven and Warburton [141].

To check the convergence rate, we construct the following exact solutions for the 2-D TM model (assuming that $\Gamma_m = \Gamma_e = \omega_m = \omega_e = 1$) on domain $\Omega = (0,1)^2$:

$$\mathbf{H} \equiv \begin{pmatrix} H_x \\ H_y \end{pmatrix} = \begin{pmatrix} \sin(\omega\pi x)\cos(\omega\pi y)\exp(-t) \\ -\cos(\omega\pi x)\sin(\omega\pi y)\exp(-t) \end{pmatrix},$$

$$E_z = \sin(\omega\pi x)\sin(\omega\pi y)\exp(-t).$$

The corresponding magnetic and electric currents are

$$\mathbf{K} \equiv \begin{pmatrix} K_x \\ K_y \end{pmatrix} = \begin{pmatrix} t\sin(\omega\pi x)\cos(\omega\pi y)\exp(-t) \\ -t\cos(\omega\pi x)\sin(\omega\pi y)\exp(-t) \end{pmatrix},$$

and

$$J_z = t\sin(\omega\pi x)\sin(\omega\pi y)\exp(-t),$$

respectively. The corresponding source term

$$f = (t - 1 - 2\omega\pi)\sin(\omega\pi x)\sin(\omega\pi y)\exp(-t),$$

while $\mathbf{g} = (g_x, g_y)'$ is given by

$$g_x = (\omega\pi - 1 + t)\sin(\omega\pi x)\cos(\omega\pi y)\exp(-t),$$
$$g_y = (1 - \omega\pi - t)\cos(\omega\pi x)\sin(\omega\pi y)\exp(-t),$$

Notice that E_z satisfies the boundary condition $E_z = 0$ on $\partial\Omega$.

The function *MetaRHS2D.m* is used to evaluate the right-hand-side flux in the 2-D TM form. Its detailed implementation is shown below:

```
function [rhsHx, rhsHy, rhsEz] = MetaRHS2D(Hx,Hy,Ez)
% Purpose: Evaluate RHS flux in 2D Maxwell TM form
```

```
Globals2D;

% Define field differences at faces
dHx = zeros(Nfp*Nfaces,K); dHx(:) = Hx(vmapM)-Hx(vmapP);
dHy = zeros(Nfp*Nfaces,K); dHy(:) = Hy(vmapM)-Hy(vmapP);
dEz = zeros(Nfp*Nfaces,K); dEz(:) = Ez(vmapM)-Ez(vmapP);

% Impose reflective boundary conditions (Ez+ = -Ez-)
dHx(mapB) = 0; dHy(mapB) = 0; dEz(mapB) = 2*Ez(vmapB);

% upwind flux (alpha = 1.0); central flux (alpha = 0.0);
alpha = 1.0;
ndotdH =  nx.*dHx+ny.*dHy;
fluxHx =  ny.*dEz + alpha*(ndotdH.*nx-dHx);
fluxHy = -nx.*dEz + alpha*(ndotdH.*ny-dHy);
fluxEz = -nx.*dHy + ny.*dHx - alpha*dEz;

% local derivatives of fields
[Ezx,Ezy] = Grad2D(Ez);
[CuHx,CuHy,CuHz] = Curl2D(Hx,Hy,[]);

% compute right hand sides of the PDE's
rhsHx = -Ezy  + LIFT*(Fscale.*fluxHx)/2.0;
rhsHy = Ezx  + LIFT*(Fscale.*fluxHy)/2.0;
rhsEz =  CuHz + LIFT*(Fscale.*fluxEz)/2.0;

return;
```

The function *Meta2D.m* is used to perform the time-marching using a classic low-storage five-stage fourth-order explicit Runge-Kutta method. The code *Meta2D.m* is shown below:

```
function [Hx,Hy,Ez,Kx,Ky,Jz,time] = ...
         Meta2D(Hx,Hy,Ez,Kx,Ky,Jz,x,y,FinalT)

% Purpose: Integrate TM-mode Maxwell equations until
%  FinalT starting with initial conditions Hx,Hy,Ez

Globals2D;
time = 0;

% Runge-Kutta residual storage
resHx = zeros(Np,K);
resHy = zeros(Np,K);
resEz = zeros(Np,K);
resKx = zeros(Np,K);
resKy = zeros(Np,K);
resJz = zeros(Np,K);
```

```
dt = 1e-6; omepi=4*pi;
istep=0;
% outer time step loop
while (time<FinalT)

  if(time+dt>FinalT), dt = FinalT-time; end
  f=feval(@fun_f21,x,y,time,omepi);
  gx=feval(@fun_gx21,x,y,time,omepi);
  gy=feval(@fun_gy21,x,y,time,omepi);
  for INTRK = 1:5
       rhsKx = -Kx+Hx; rhsKy = -Ky+Hy; rhsJz = -Jz+Ez;
       resKx = rk4a(INTRK)*resKx+dt*rhsKx;
       resKy = rk4a(INTRK)*resKy+dt*rhsKy;
       resJz = rk4a(INTRK)*resJz+dt*rhsJz;

      % compute RHS of TM-mode Maxwell equations
      [rhsHx, rhsHy, rhsEz] = MetaRHS2D(Hx,Hy,Ez);
      rhsHx = rhsHx-Kx+gx;
      rhsHy = rhsHy-Ky+gy;
      rhsEz = rhsEz-Jz+f;
      % initiate and increment Runge-Kutta residuals
      resHx = rk4a(INTRK)*resHx + dt*rhsHx;
      resHy = rk4a(INTRK)*resHy + dt*rhsHy;
      resEz = rk4a(INTRK)*resEz + dt*rhsEz;

      % update fields
      Hx = Hx+rk4b(INTRK)*resHx;
      Hy = Hy+rk4b(INTRK)*resHy;
      Ez = Ez+rk4b(INTRK)*resEz;
      Kx = Kx+rk4b(INTRK)*resKx;
      Ky = Ky+rk4b(INTRK)*resKy;
      Jz = Jz+rk4b(INTRK)*resJz;
   end;
   % Increment time
   time = time+dt;
   istep = istep + 1;
   disp('step, time ='), istep, time
end
return
```

The function *Meta2DDriver.m* is the driver script. The detailed implementation for our example is shown below:

```
% Driver script for 2D metamaterial equations

Globals2D;
```

```
% Polynomial order used for approximation
N = 1;

%%%%%%%%%%%%%%%%%%%%%%%%%%%%%%%%%%%%%%%%%%%%%%%%
% Generate a uniform triangular grid

nelex=20;     % number of elements in x-direction
nx = nelex+1;   % number of points in x direction
Nv = nx*nx;       % total number of grid points
K = 2*nelex*nelex;  % total number of elements
no2xy = genrecxygrid(0,1,0,1,nx,nx)';
VX = no2xy(1,:); VY=no2xy(2,:);
EToV = delaunay(VX,VY);

% Reorder elements to ensure counterclockwise order
ax = VX(EToV(:,1)); ay = VY(EToV(:,1));
bx = VX(EToV(:,2)); by = VY(EToV(:,2));
cx = VX(EToV(:,3)); cy = VY(EToV(:,3));

D = (ax-cx).*(by-cy)-(bx-cx).*(ay-cy);
i = find(D<0);
EToV(i,:) = EToV(i,[1 3 2]);

%%%%%%%%%%%%%%%%%%%%%%%%%%%%%%%%%%%%%%%%%%%%%%%%
% Initialize solver and construct grid and metric

StartUp2D;

% Set initial conditions
omepi = 4*pi;   % omega*pi always together
Hx = sin(omepi*x).*cos(omepi*y);
Hy = -cos(omepi*x).*sin(omepi*y);
Ez = sin(omepi*x).*sin(omepi*y);
Kx = zeros(Np,K); Ky=zeros(Np,K); Jz=zeros(Np,K);

% Solve Problem
FinalT = 1e2*1.0e-6;
% measure elapsed time.
tic
[Hx,Hy,Ez,Kx,Ky,Jz,time] ...
      = Meta2D(Hx,Hy,Ez,Kx,Ky,Jz,x,y,FinalT);
toc

exactHx=sin(omepi*x).*cos(omepi*y)*exp(-FinalT);
exactHy=-cos(omepi*x).*sin(omepi*y)*exp(-FinalT);
exactEz=sin(omepi*x).*sin(omepi*y)*exp(-FinalT);
exactKx=FinalT*sin(omepi*x).*cos(omepi*y)*exp(-FinalT);
exactKy=-FinalT*cos(omepi*x).*sin(omepi*y)*exp(-FinalT);
exactJz=FinalT*sin(omepi*x).*sin(omepi*y)*exp(-FinalT);

errorHx = max(max(abs(Hx-exactHx))),
errorHy = max(max(abs(Hy-exactHy))),
errorEz = max(max(abs(Ez-exactEz))),
errorKx = max(max(abs(Kx-exactKx))),
```

```
errorKy = max(max(abs(Ky-exactKy))),
errorJz = max(max(abs(Jz-exactJz))),

figure(1)
quiver(x,y,Hx,Hy);
title('numerical magnetic field');
tri = delaunay(x,y);
figure(2)
quiver(x,y,exactHx,exactHy);
title('analytic magnetic field');

figure(3)
trisurf(tri,x,y,Ez);
title('Numerical electric field');
figure(4)
trisurf(tri,x,y,Ez-exactEz);
title('Pointwise error of electric field');

figure(5)
trisurf(tri,x,y,Jz);
title('Numerical induced electric current');
figure(6)
trisurf(tri,x,y,Jz-exactJz);
title('Pointwise error of induced electric current');
```

Of course, to solve our example, we need three supporting MATLAB functions *fun_f21.m, fun_gx21.m, fun_gy21.m* to evaluate functions f, g_x and g_y, respectively. Also we need a mesh generator function *genrecxygrid.m*.

The code *fun_f21.m* is shown below:

```
function val=fun_f21(x,y,t,omepi)

val =(t-1-2*omepi)*exp(-t)*sin(omepi*x).*sin(omepi*y);
```

The code *fun_gx21.m* is shown below:

```
function val=fun_gx21(x,y,t,omepi)

val =(omepi+t-1)*exp(-t)*sin(omepi*x).*cos(omepi*y);
```

The code *fun_gy21.m* is shown below:

```
function val=fun_gy21(x,y,t,omepi)

val =(1-omepi-t)*exp(-t)*cos(omepi*x).*sin(omepi*y);
```

The code *genrecxygrid.m* is shown below:

```
% generate a square grid of points on the xy-plane
% Inputs:
%    Domain [xlow,xhigh]x[ylow,yhigh]
%    xn, yn: number of points in the x- and y-directions.

function [xy] = genrecxygrid(xlow,xhigh,ylow,yhigh,xn,yn)
```

Table 4.1 The L^∞ errors with $\tau = 10^{-6}$, $Nr = 1$ at 100 time step

Errors	$h = 1/10$	$h = 1/20$	$h = 1/40$	$h = 1/80$	$h = 1/160$
Hx	0.0013	7.3433e−004	3.8435e−004	1.9291e−004	9.5417e−005
Hy	0.0013	7.3433e−004	3.8435e−004	1.9291e−004	9.5417e−005
Ez	0.0021	0.0011	5.7637e−004	2.8954e−004	1.4261e−004
Kx	6.4776e−008	3.6787e−008	1.9283e−008	9.7061e−009	4.8216e−009
Ky	6.4776e−008	3.6787e−008	1.9283e−008	9.7061e−009	4.8216e−009
Jz	1.0302e−007	5.4335e−008	2.8892e−008	1.4562e−008	7.2149e−009

Table 4.2 The L^∞ errors with $\tau = 10^{-6}$, $Nr = 2$ at 100 time step

Errors	$h = 1/5$	$h = 1/10$	$h = 1/20$	$h = 1/40$	$h = 1/80$
Hx	0.0018	5.9136e−004	1.5830e−004	4.0508e−005	1.0099e−005
Hy	0.0018	5.9136e−004	1.5830e−004	4.0508e−005	1.0100e−005
Ez	0.0022	7.1938e−004	1.9800e−004	5.0975e−005	1.2856e−005
Kx	8.9076e−008	2.9593e−008	7.9259e−009	2.0324e−009	5.0834e−010
Ky	8.9076e−008	2.9593e−008	7.9259e−009	2.0324e−009	5.0834e−010
Jz	1.1244e−007	3.6006e−008	9.9139e−009	2.5500e−009	6.4321e−010

```
xorig=[linspace(xlow,xhigh,xn),linspace(ylow,yhigh,yn)];
n  = xn*yn;
xy = zeros(n,2);     % x,y coordinates of all points
pt = 1;
for j = 1:yn
   for i = 1:xn
      xy(pt,:)=[xorig(i) xorig(xn+j)];
      pt=pt+1;
   end
end

return
```

With these MATLAB functions, we can solve this example on uniformly refined meshes with various time step sizes τ and different orders Nr of polynomial basis functions. Exemplary results are shown in Tables 4.1 and 4.2, which justify the following convergence result:

$$\max_{m\geq 1}(||\mathbf{H}^m - \mathbf{H}_h^m||_{L^\infty(\Omega)} + ||\mathbf{E}^m - \mathbf{E}_h^m||_{L^\infty(\Omega)} + ||\mathbf{J}^m - \mathbf{J}_h^m||_{L^\infty(\Omega)} + ||\mathbf{K}^m - \mathbf{K}_h^m||_{L^\infty(\Omega)}) \leq C h^{Nr}.$$

Exemplary solutions for E_z and the corresponding pointwise errors obtained with $Nr = 2, \tau = 10^{-6}$ at 100 time steps are presented in Fig. 4.1. More numerical results using the package *nudg* of [141] can be found in Li [185].

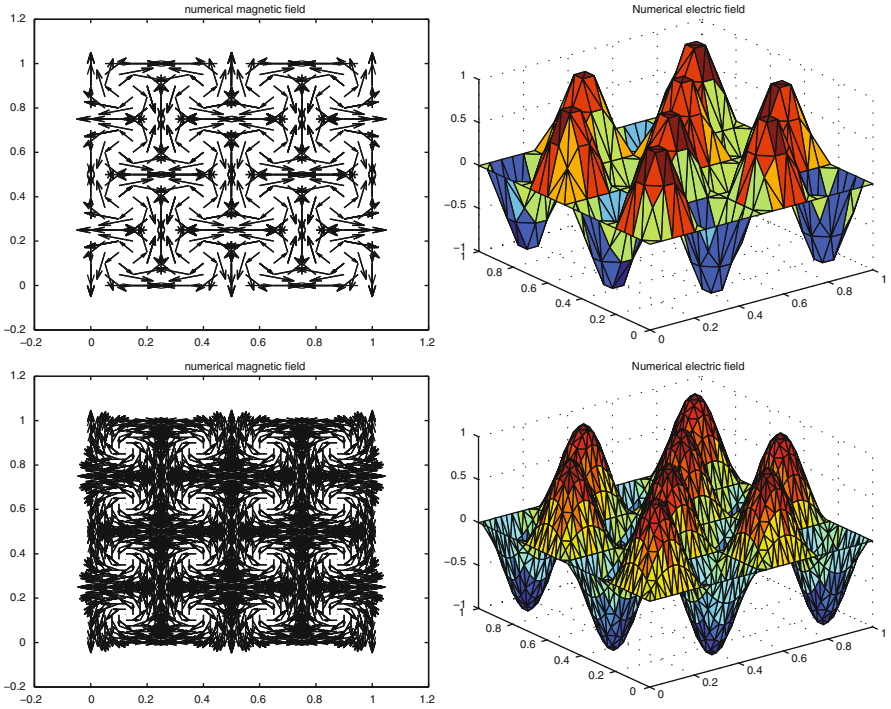

Fig. 4.1 Results obtained with $Nr = 2, \tau = 10^{-6}$ at 100 time steps. *Top row* (with $h = 1/10$): magnetic field H (*Left*) and electric field E (*Right*); *bottom row* (with $h = 1/20$): magnetic field H (*Left*) and electric field E (*Right*)